Sulfurization of near-stoichiometric CuIn-precursor and the influence of low-temperature-slopes on morphology and structural quality

Authors: A. Dombrowa, C. Lehmann, C. Pettenkofer
Corresponding author: Christian Pettenkofer email: pettenkofer@helmholtz-berlin.de

Keywords: CIS, $CuInS^2$, XPS/UPS, XRD, SEM, EDX, sulfurization, Cu/In-ratio of 1.2, near-stoichiometric precursor, morphology, crystal quality

Abstract

Polycrystalline $CuInS_2$ (CIS) films are prepared by sulfurization of CuIn metallic precursors with Cu/In=1.2 on Mo substrates. Variation of the rapid thermal processing (RTP) parameters adjusted to the low Cu surplus yielded near stoichiometric CIS films with considerably less CuS_x precipitation at the surface. A start temperature and low temperature slopes were introduced to guarantee crystal quality and large grain size. XPS/UPS, XRD and SEM data show the distinct properties of the chalcopyrite phase and its morphological structure in comparison to the standard sulfurization process. A considerable improvement has been achieved by variation of the temperature profiles. The proposed process modules obtain near stoichiometric CIS films for industrial solar cell production.

Introduction

Polycrystalline $CuInS_2$ is applied as absorber material in thin film solar cells. Of various methods of preparation the sulfurization of a metallic precursor has been established as the standard process for industrial production [1],[2],[3]. In the past details of the chemical reactions during sulfurization and the effects on photovoltaic applications have been investigated [4],[5],[8],[10],[11],[12]. It was demonstrated [4][7], that the sulfurization process is dominated by boundary diffusion and therefore correlated to stress-induced growth that occurs only during temperature slopes.

To convert the metastable Cu-Au-ordered $CuInS_2$ phase (CA), into chalcopyrite ordering (CH), a temperature of about 500°C is necessary [4],[5],[8]. A near-stoichiometric or In-rich precursor leads to amounts of secondary phases ($CuIn_5S_8$, Cu-Au-ordered domains) resulting in a lower performance due to donor like defects [9], [13], [9]. Therefore p-doped $CuInS_2$ is obtained at industrial baselines by sulfurization of metallic CuIn-precursor with Cu:In ratio of 1.4 to 1.6. in a rapid thermal process (RTP) featuring a temperature profile as shown in Fig. 1(a). It is known, that Cu_xS (x=1,2) phases, obtained by Cu-excess, act as a fluxing agent during the $CuInS_2$ formation thereby effectively reducing donor-like defects which are basically sulfur vacancies and In_{Cu}-antisites [11],[10],[9],[4],[5]. The excess CuS segregates at the surface which can be removed by KCN etching.

Avoiding the segregation and thereby the ex-situ KCN etching process would enable an in-line process including the deposition of the TCO-layer completely under vacuum conditions. To end up with an CuS free absorber surface, it is necessary to sulfurize samples with only a small amount of Cu surplus just sufficient to ensure the intrinsic p-type-doping. However, the absence of a large copper surplus impairs the structural and crystal quality which must be compensated [6],[4],[5].

Therefore the experiments below have been designed in order to achieve a small amount of CuxS formation and its benefits during the low-temperature part of the sulfurization in spite of using near-stoichiometric precursors with reduced copper surplus. This is feasible regarding the Cu-In-quantities of the compounds involved below 300°C. Completing the final stage of the sulfurization and adding a post-growth heat treatment yields an absorber without CuS.

Experimental:

Sulfurization, thermal treatment and the XPS/UPS characterization of the samples were performed in a dedicated ultra high vacuum system. The Cu/In-precursors were prepared on molybdenum substrates. Prior to the precursor layer deposition the Mo-substrate was coated with a sputtered Mo-layer of 500 nm to provide an uncontaminated and smooth surface akin to those commercially prepared on glass substrates. A metallic bi-layer of industrial standard thickness consisting of 352nm Cu and 648nm In was deposited by sequential sputtering, performed at the HZB baseline at a base pressure of $6x10^{-8}$ mbar. The Cu/In ratio of 1.2 is significantly closer to stoichiometry than the Cu/In ratio of >1.4 commonly used. The samples were transported ex-situ and cleaned after introduction into the UHV-system by annealing at 550°C for 2h. After thermal cleaning the CuIn-precursor consists mainly of $Cu_{11}In_9$ alloy coexisting with a crystalline In phase [14], [4],[5]. The sulfurization of the CuIn-precursor was performed in a dense sulfur atmosphere attained by evaporation of elementary sulfur at about 120°C. In contrast to the common rapid thermal process (RTP) a thermocouple controlled resistance heating system allowed for a controlled thermal process with several sophisticated temperature profiles. The temperature profile was adjusted to exploit the reactive phase transitions of the sulfurization process involving CuS. To facilitate grain boundary diffusion by thermal strain the ascending slopes were run at a rate of 15°C per minute. After the sulfurization process the samples were annealed for another hour at 550°C in the absence of sulfur. This post-sulfurization heat-treatment completes the process by enabling additional phase transitions, diffusion and an improvement of the structural properties as reported in various studies [15], [16].

The samples were investigated in-situ by photoelectron spectroscopy using a Phoibos 150 analyzer with a MCD-9 detector, a XR-50 X-ray source Mg K alpha (1253.6 eV) and He-I lamp (21.2 eV). In order to supplement the surface-sensitive data, ex-situ volume-sensitive x-ray diffraction measurements (XRD) and energy dispersive x-ray analysis (EDX) were carried out. The crystal structure and phase composition were investigated with standard XRD measurements in a theta-2theta geometry performed in a D8 Advance (Bruker AXS) diffractometer with excitation by Cu-K-$alpha_{1,2}$. The diagrams were recorded in the range of 10° to 120° with an increment of 0.005°. The chemical composition of the volume was analyzed by EDX. Elemental mappings

were obtained from an area of 40x50 µm^2 and a depth of 500 nm (10 kV measurements). Scanning electron microscopy analysis (SEM) was performed to gain further knowledge of the surface morphology as well as the grain size. The electron beam energy was 25keV while the scanned area shown in Fig. 4 was 30x40 µm^2.

Results and discussion:

Three groups of samples were prepared.

Sample I

For reference a sample was sulfurized utilizing a temperature profile well-established at commercial baselines (Fig. 1(a)). This profile consists of a temperature slope up to about 500°C while the sample is exposed to the S atmosphere. After a dwelling time of 10min the sample is cooled down.

Sample II

To avoid the formation of InS from superficial In and S which is considered to be a precursor of the unwanted $CuIn_5S_8$ phase, sample II was heated to a starting temperature prior to exposure to the sulfur atmosphere as shown in Fig. 1(b). The start temperature of 175°C was chosen well above the melting point of In at vacuum conditions (160°C). At this temperature segregated In agglomerates have been liquefied and have completely reacted with Cu forming $Cu_{11}In_9$ alloy [4],[5].

Sample III

For sample III further modifications of the sulfurization profile were based on the formation of $CuInS_2$ out of the $Cu_{11}In_9$ phase at temperatures of 200°C to 300°C [4],[5]. To extend the sulfurization process within this temperature range alternating increasing and decreasing low-temperature-slopes were performed (Fig. 1(c)). At 300°C the phase transition of $Cu_{11}In_9$ into $Cu_{16}In_9$ takes places [4],[5]. This is accompanied by the release of an amount of In which in our case cannot be bound by excess Cu. The formation of InS by unbound In becomes possible. Since the InS phase is the point of origin of an unfavourable reaction path its formation must be prevented [5],[8]. The variation of the temperature from 175°C to 250°C serves this purpose as it allows a sufficient amount of surface $CuInS_2$ and Cu_xS (x=1,2) to form shielding the In from the sulfur atmosphere.

pre treatment:

After thermal cleaning XPS investigations yield a negligible carbon signal and oxygen impurities below the detection limit of XPS. The XRD measurements of the metallic precursor exhibit a dominating $Cu_{11}In_9$ alloy signal accompanied with smaller signals of In crystallites. Taking into account the molecular factor of m=-0.6 derived from XPS an In-rich surface can be assumed and In crystals at least partially reside on the surface. This corresponds to the results of Gossla [14].

Sulfurization and post-process heating

A VBM of about 0.7 eV - 0.8 eV is expected for stoichiometric $CuInS_2$, whereas a VBM of higher values indicate n-type $CuInS_2$ featuring donor-type defects like In_{Cu}, V_S or V_{Cu} (Fig. 2(a)/(b)). The chalcopyrite structure is revealed by characteristic peaks at 27.9°, 32.3° and 46.4° corresponding to the (112), (004)/(200) and (204)/(220) reflections (Fig. 3). Moreover, this is backed up by $CuInS_2$ signals at 55.0°, 74.8° and 86.1° (not shown) referring to the (116)/(312), (316)/(332) and (228)/(424) reflections, which also correspond to $CuInS_2$. A distinct splitting of the (004)/(200) and (204)/(220) reflections indicates the chalcopyrite's tetragonal distortion. Fig. 4(a) shows the SEM picture of sample II with the introduction of the start-temperature, while Fig. 4(b) documents the application of combined start-temperature and low-temperature-slopes of sample III.

Sample I:

After sulfurization, sample I (Fig.2(a)) shows $CuInS_2$ valence band structure [20],[17]. However, the sample features a lower intensity of the Cu3d-DOS (density of states) and a VBM in the range of n-type $CuInS_2$. These observations match the Cu- and S-poor stoichiometry derived from XPS-data. The Auger-parameter of Cu and In is in the range of $CuInS_2$. No phase transformation can be derived from the XPS/UPS spectra (Fig.2(b)) after post-processing heating. However, taking into account the shift of the VBM a Cu-diffusion from the volume can be assumed. The shift is probably caused by less V_{Cu} and In_{Cu} defects and accompanied by the slightly increased Cu-states in the valence band respectively. Furthermore, the stoichiometry has changed to less Cu-poor values.

The XRD-spectra of sample I indicate additional phases corresponding to Cu_xIn_y-phases. Sample I exhibits a low reflection splitting due to CuAu-ordering which is caused by a high density of defects thus indicating a poor crystalline quality.

The elemental distribution measured by EDX shows a general Cu- and S- deficiency with small inhomogeneous spots of increased Cu and S deficiency. This deficiency is confirmed by XPS data implying an even more Cu- and S-deficient surface.

Sample II:

Sample II prepared with initial annealing shows the VB-structure of CuS with a VBM at the Fermi level according to the p-metal characteristic of CuS. The appearance of a second phase at the Cu2p and S2p XPS peaks indicates a superposition of $CuInS_2$ and CuS spectra. This assumption is supported by the binding energies of the identifiable sulfur phases and the Auger-parameters of Cu and In which correspond to $CuInS_2$ as well as CuS. With respect to the main Cu phase, the Auger-parameter indicates CuS whereas the Auger-parameter of In is in the range of $CuInS_2$. The stoichiometry is Cu- and S-rich. After post-sulfurisation heating sample II shows the typical VB-structure of $CuInS_2$. Furthermore, no secondary phases can be detected by XPS. Sample II features a VBM at 1.0 eV, low Cu-DOS and a more In-rich stoichiometry indicating n-type $CuInS_2$. The change from a Cu-rich to a Cu-poor surface implies that non-sulfurized residues of the metallic precursor have reacted with a small superficial amount of CuS. The XRD results reveal values between that of sample I and III. The secondary Cu_xIn_y phase is reduced and the $CuInS_2$ phase is increased but the crystalline quality remains poor compared to sample III described below. The SEM picture of sample II shows a

rough surface with a droplet-like appearance and a small grain size as indicated by the FWHM of the (112) XRD-reflex.

Sample III:

After sulfurization, the UPS/XPS spectra of sample III are identical with sample II, but shows differences after post-sulfurisation heating. In contrast to sample I and II, sample III shows a valence band structure with well pronounced Cu3d-DOS combined with a VBM at 0.8 eV and stoichiometric composition derived from XPS-data. According to NIST data base [18] the derived Cu-Auger-parameter of 1849.4 lies between that of $CuInS_2$ (1848.9-1849.1) and Cu_2S (1849.6-1849.9). This either indicates Cu-rich $CuInS_2$ or a superposition of $CuInS_2$ and Cu_2S. The XRD spectrum corresponding to sample III shows a distinct single $CuInS_2$ signal.

The Cu_xIn_y -signals were absent for sample III and phases like In_xS or $CuIn_5S_8$ can be excluded. Comparing sample I, II and III the intensity of the $CuInS_2$ (112) diffraction peak increases from sample I to sample III. An analysis of the (112)-$CuInS_2$ reflexes by Voigt profiles yields that sample III features the sharpest peaks. The reduction of the FWHM from 0.22°(sample I) via 0.18 (sample II) to 0.14° (sample III) can be attributed to an increased average grain size as deduced by the Scherrer formula [19] and is supported by the SEM images (Fig. 4). A distinct peak-splitting can be observed only on sample III.

The SEM picture reveals that the surface is dense and smooth with compact grains of sizes of 1-2 µm. Only few occasional residuals are segregated. EDX exhibits areas of relative Cu as well as Cu and S surplus. These larger inhomogeneous regions indicate CuS or Cu_2S-residues. The surface morphology in general can be attributed to the $CuInS_2$ phase since a significant covering Cu_xS (x=1,2) phase can be ruled out by the XPS/UPS data.

The $Cu_{11}In_9$ phase can be regarded as an ideal start condition for sulfurization since its composition is close to the 1:1 stoichiometric ratio of the metallic components of the compound $CuInS_2$. However, agglomerations of In crystallites on the surface cause the undesirable formation of InS and must be therefore prevented during the sulfurization process.

CuS is a potential fluxing agent for the sulfurization. We assume that the Cu_xIn_y phases revealed by the XRD spectra of sample I and II originate from an incomplete sulfurization process arising from the absence of CuS during the process. Adding sulfur at start-temperature of 175°C where segregated In agglomerates are liquefied and have completely reacted with Cu forming $Cu_{11}In_9$ leads to an improvement but is not sufficient with regard to the absorber quality.

However, sample III contained enough CuS during the process to obtain stoichiometric $CuInS_2$ by post-process heating. The required CuS is yielded by low-temperature-slopes prior to the high temperature part of the sulfurization. This could be shown by a precursor which was processed up to the low-temperature-slopes and subsequently cooled down without processing in the high temperature region. It yielded a thick (>500nm) initial CuS-layer verified by XRD, EDX and XPS/UPS. Furthermore, the $CuInS_2$ formation in the low-temperature region could be proven by XRD (not shown) [21].

Since post-sulfurization heating was performed devoid of sulfur atmosphere, chemical reactions must be assumed to have been taken place between the surface and the bulk. The phase transition of CuS to Cu_2S is known to take place at about 500°C while the reverse transformation Cu_2S to CuS only takes place when sulfur is supplied [4]. It is likely that a transformation to Cu_2S is a minor side process during the post-processing of sample III. While a CuS phase can be excluded by XRD, Cu_2S x-ray reflections are not easily distinguished from the $CuInS_2$ reflections and may be indiscernible in XRD spectra. Since Cu_2S is a semiconductor of similar band gap as $CuInS_2$, residuals of Cu_2S would be likewise indiscernable at the VBM, especially since the stoichiometry of the sample implies that the Cu_2S residuals are of a minor amount. Therefore Cu_2S-residuals are an explanation for the Cu-rich areas revealed by EDX and probably match with the residuals seen in the SEM picture.

The increased intensity of the (112) XRD-reflex and the absence of other phases at sample III indicate that the extent of $CuInS_2$ formation is improved by the afore mentioned start temperature of 175°C but mainly by the added low-temperature-slopes. The slopes allow $CuInS_2$ and Cu_xS formation by means of stress-induced growth while Cu_xS supports further formation of $CuInS_2$. Furthermore, the distinct reflection splitting and the narrowing of the FWHM indicate the formation of $CuInS_2$ with higher crystalline quality. Sample III yields a compact surface morphology and increased grain size which is supported by SEM and XRD. This improvement is the result of three effects: 1) the reaction path and the intermediate reaction products have an impact on aspects like augmented insertion of sulfur via Cu_xS leading to reduced sulfur vacancies, 2) the sulfurization progress is aided by the fluxing agent Cu_xS and impeded by InS and 3) the grain size is small along the InS-In_2S_3-$CuIn_5S_8$-$CuInS_2$ reaction path and is increased along the CuS-$CuInS_2$ path [4],[6].

Table I: Summary of the key data for sample I through III derived from XPS/UPS data.

post heating data	Sample I	Sample II	Sample III
VBM	1.2 eV	1.0 eV	0.8 eV
W_f	4.8 eV	4.9 eV	5.3 eV
Δm=Cu/In-1	-0.63	-0.40	-0.05
Δs=2S/(Cu+3In)-1	-0.13	-0.05	-0.01
αCu †	1849.1	1849.1	1849.4
αIn ††	825.4	852.5	852.5

† *αCu = binding energy ($Cu2p_{3/2}$) + kinetic energy (CuMM)*
†† *αIn = binding energy ($In3d_{5/2}$) + kinetic energy (InMNN)*

Conclusion

To expand the two-stage sulfurization process onto metallic precursors with a Cu/In ratio of 1.2, the process window in the temperature range below 300°C has been exploited. The results of the samples I, II and III, each sulfurized with identical CuIn-precursor set-up but different process modules, show the influence of the preparation process on the reactive formation of the crystal.

We have demonstrated that the crystalline and structural properties of the CIS absorber can be improved by inhibiting the growth path including InS as intermediate reaction product and simultaneously enhancing the initial CuS formation, known to be beneficial for the reactive process. Two new process modules avoid unbound In at the precursor surface and instead provide Cu for Cu_xS (x=1,2) formation. Firstly, we choose a start-temperature of 175°C which provides a precursor completely composed of the alloy $Cu_{11}In_9$. Secondly, low-temperature-slopes exploit the formation of $CuInS_2$ from $Cu_{11}In_9$ alloy creating a slight overrun of Cu and simultaneously avoiding the phase-transition from $Cu_{11}In_9$ to $Cu_{16}In_9$ In at 300°C.
The released Cu is able to react at the surface with sulfur forming the beneficial Cu_xS (x=1,2) phase and $CuInS_2$ as proven by a sample processed only up to the low-temperature-slopes. Thus, the introduced modules provide Cu_xS even for Cu/In-ratio of 1.2. The formation of In-rich $CuInS_2$ or rather In-rich defect complexes, which normally take place in the range of small Cu/In-ratios, can probably be suppressed providing a surface with a minimized density of defects.
The process adapted to 1.2 precursor leads to well-crystallized films of chalcopyrite ordered $CuInS_2$, forming large grains and a smooth surface with only little Cu_xS residues remaining on the surface. The residues consist probably of Cu_2S. The post-sulfurization heat treatment causes recrystallization, thereby improving the crystallinity [15],[9]. Moreover, it enables the reaction of segregated CuS with the volume thus converting superficial CuS into further $CuInS_2$ and a small amount of Cu_2S residua. At the end of the process no CuS is left. Although it could not be shown whether the Cu_2S-residuals have to be removed by KCN etching, the new process modules could be a promising way to produce CIS absorber for photovoltaic applications.
It is recommended that further studies using precursors with Cu/In=1.0 or 1.1 should be conducted in order to avoid Cu_2S-residuals altogether. The results should enable to prepare the $CuInS_2$ to buffer-layer heterojunction in a complete vacuum in-line process and therefore minimize impurities and potentially augment the solar cell efficiency.

Acknowledgment
The authors would like to thank their colleagues of HZB for their skillful support, in particular J. Klaer for kindly preparing the CuIn-precursor, Dr. G. Zehl for the XRD measurements and C. Klimm for the SEM/EDX investigations.

References
[1] Proceedings of the 22nd European Photovoltaic Solar Energy Conference and Exhibition, Milan. A. Meeder, A. Neisser, U. Rühle, N. Meyer, 2007.
[2] J. Klaer, I. Luck, A. Boden R. Klenk I. Gavilanes Perez R. Scheer. Thin Solid Films, 431-432:534–537, 2003.
[3] N. Meyer, I. Luck, U. Rühle; J. Klaer; R. Klenk M. Ch. Lux-Steiner R. Scheer. Proceedings of the 19th European Photovoltaic Solar Energy Conference and Exhibition, Paris, 4AO.:9.6, 2004.
[4] J. Djordjevic, Ch. Pietzker, R. Scheer. Journal of Physics and Chemistry of Solids, 64:p.1843-1848, 2003.
[5] E. Rudigier, Ch. Pietzker, M.Wimbor, I. Luck, J. Klaer, R. Scheer, B. Barcones, T. Jawhari Colin, J. Alvarez-Garcia, A. Perez-Rodriguez, A. Romano-Rodriguez. Thin Solid Films 431-432:p.110-115, 2003.
[6] E. Rudigier, J. Alvarez-Garcia, I. Luck, J. Klaer, R. Scheer. Journal of Physics and Chemistry of Solids, 64:p.1977-1981, 2003.
[7] E. Rudigier, J. Djordjevic, C. von Klopmann, B. Barcones, A. Pérez-Rodriguez, R. Scheer. Journal of Physics and Chemistry of Solids, 66:p.1954-1960, 2005.
[8] Ch. von Klopmann, J. Djordjevic, E. Rudigier, R. Scheer. Journal of Cryсstal Growth, 289:121-133, 2006.
[9] J. Alvarez-Garcia, E. Rudigier, N. Rega, B. Barcones, R. Scheer, A. Pérez-Rodriguez, A. Romano-Rodriguez, J.R.Morante. Thin Solid Films, 431-432:p.122-125, 2003
[10] E. Rudigier, T. Enzenhofer, R. Scheer. Thin Solid Films 480-481:327-331, 2005.
[11] S. Merdes, R. Mainz, H. Rodriguez-Alvarez, J. Klaer, R. Klenk, A. Meeder, H.W. Schock, M.Ch. Lux-Steiner. Thin Solid Films, in press, 2011.
[12] D. Thomas, R. Mainz, H. Rodriguez-Alvarez, B. Marsen, D. Abou-Ras, M. Klaus, Ch. Genzel, H.W. Schock. Thin Solid Films, in press, 2011.
[13] J. Eberhardt, J. Cieslak, H. Metzner, Th. Hahn, , R. Goldhahn, F. Hudert, J. Kräußlich, U Kaiser, A. Chuvilin, U. Reislöhner, W. Witthuhn. Thin Solid Films 517:2248-2251, 2009.
[14] M. Gossla, H. Metzner, E. Mahnke. Journal Of Applied Physics, 86:3624–3632, 1999.
[15] Y.B.He, T.Krämer, I.Österreicher B.K.Meyer M.Hardt. Semicond. Sci. Technol., 20 No 8:685–692, 2005.
[16] I. Oja, N. Nanu, A. Katerski M. Krunks A. Mere L. Raudoja A. Goossens. Thin Solid Films, 480-481:82–86, 2005.
[17] T. Yamamoto, H. Katayama-Yoshida, 35 L1562 (1996). Jpn. J. Appl. Phys., 35:1562, 1996.
[18] C. D. Wagner, A. V. Naumkin, A. Kraut-Vass, J. W. Allison, C. J. Powell, and John R. Rumble Jr.
National Institute of Standards and Technology, *NIST X-ray Photoelectron Spectroscopy Database 20, Version 3.5*, Website: http://srdata.nist.gov/xps/ , NIST (2003).
[19] Warren, B. E.. Dover Publ., 1990.
[20] Stefan Andres, Carsten Lehmann, Cristian Pettenkofer. Thin Solid Films, 518: 1032-1035, 2009.
[21] Dombrowa, A. Humboldt-Universität zu Berlin, 2010.

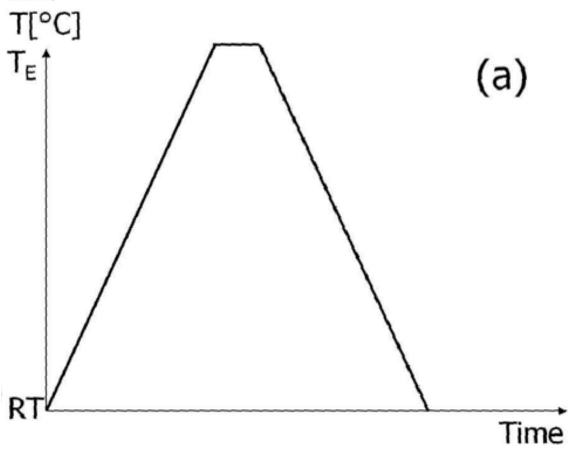
T[°C]
T_E
(a)
RT
Time

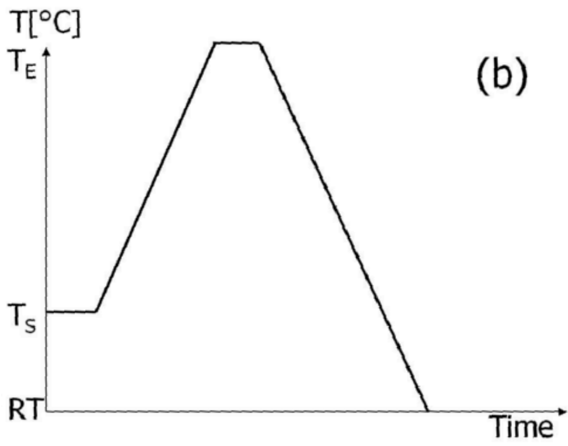
T[°C]
T_E
(b)
T_S
RT
Time

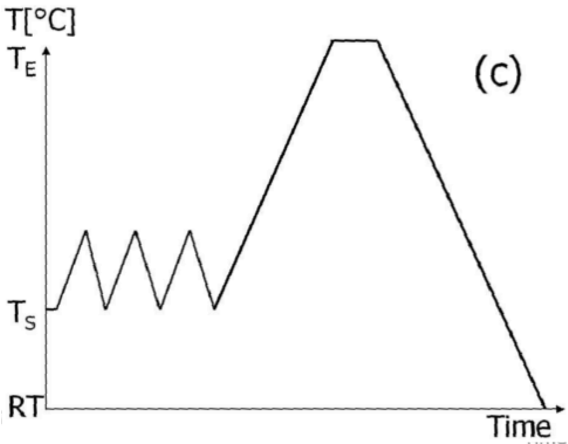
T[°C]
T_E
(c)
T_S
RT
Time

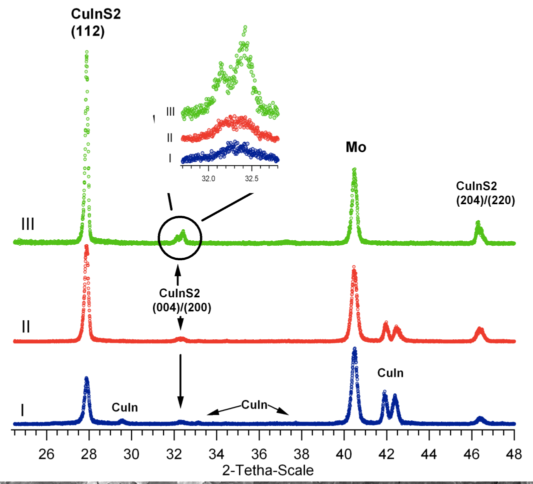
CuInS2
(112)
Mo
CuInS2
(204)/(220)
CuInS2
(004)/(200)
CuIn
III
II
I
2-Tetha-Scale

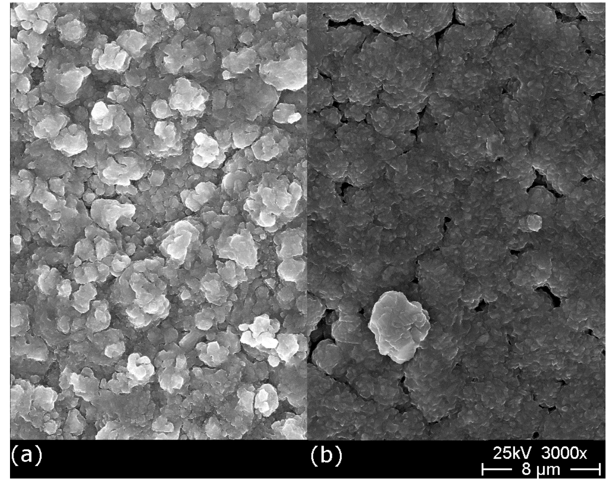
(a)
(b)
25kV 3000x
8 µm

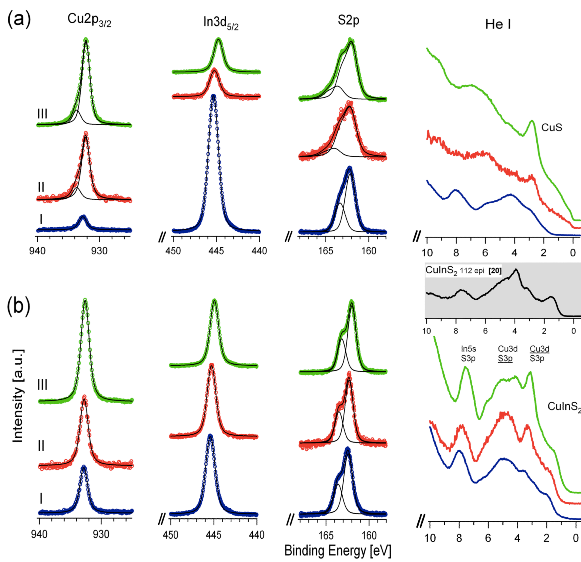
(a)
(b)
Cu2p3/2
In3d5/2
S2p
He I
CuS
CuInS2
Intensity [a.u.]
Binding Energy [eV]